Matching between regional coronary vasodilator capacity and corresponding circumferential strain in individuals with normal and increasing body weight

Gabriella M. Vincenti, MD,[a] Giuseppe Ambrosio, MD, PhD,[b] Jean-Noël Hyacinthe, MD,[c] Alessandra Quercioli, MD,[a] Yann Seimbille, MD,[c] François Mach, MD,[a] Osman Ratib, MD,[c] Jean-Paul Vallée, MD,[c] and Thomas H. Schindler, MD[a]

Background. **To define the relationship between regional coronary vasodilator capacity and myocardial circumferential strain at rest in normal weight, overweight, and obese individuals with normal global left-ventricular function.**

Methods and Results. **Myocardial blood flow at rest and during pharmacologic vasodilation was measured with ^{13}N-ammonia PET/CT in mL/g/minute in normal weight control (CON, n = 12), overweight (OW, n = 10), and obese individuals (OB, n = 10). In addition, resting myocardial function was evaluated as circumferential strain (Ɛc, %) by MRI. Global myocardial flow reserve (MFR) did not differ significantly between CON and OW (2.98 ± 0.96 vs 2.70 ± 0.66, *P* = .290), whereas it declined significantly in OB (1.98 ± 1.04, *P* = .030). Further, global Ɛc (%) was comparable between CON, OW, and OB (−0.24 ± 0.03, −0.23 ± 0.02, and −0.23 ± 0.04) but it was lowest in OB when normalized to the rate-pressure product (NƐc: −0.31 ± 0.06, −0.32 ± 0.05, and −0.26 ± 0.08). When MFR of the three major coronary territories was correlated with corresponding Ɛc, a positive association was observed in CON (*r* = 0.36, *P* = .030), in OW (*r* = 0.54, *P* = .002), and also in OB when relating NƐc to coronary vascular resistance during pharmacologic vasodilation (*r* = −0.46, *P* = .010).**

Conclusions. **Higher coronary vasodilator capacity is related to corresponding regional circumferential strain at rest in non-obese individuals, while this is also observed for reduced MFR in obesity. (J Nucl Cardiol 2012;19:693–703.)**

Key Words: Coronary circulation • myocardial blood flow • myocardial function • magnetic resonance imaging • obesity • positron emission tomography

INTRODUCTION

Normal coronary circulatory function has been widely appreciated to ascertain important antiatherosclerotic and antithrombotic effects mainly via flow-mediated and endothelium-dependent release of nitric oxide.[1] Cardiovascular risk factors such as arterial hypertension, hypercholesterolemia, smoking, diabetes mellitus, and obesity may impair a proper functioning of the coronary circulation function.[1] The identification of an abnormal coronary circulatory function has been

From the Division of Cardiology, Nuclear Cardiology and Cardiac PET/CT, Department of Specialities in Medicine,[a] Divisions of Nuclear Medicine and Radiology, Department of Medical Imaging and Information Science,[c] University Hospital of Geneva, Geneva, Switzerland; and Division of Cardiology, School of Medicine,[b] University of Perugia, Perugia, Italy.

Financial support: Research Grants 3200B0-122237 from the Swiss National Science Foundation (SNF), with contributions of the Clinical Research Center, University Hospital and Faculty of Medicine, Geneva and the Louis-Jeantet Foundation, Swiss Heart Foundation, and Fellowship Grants from the European Society of Cardiology (ESC) and the Italian Society of Cardiology (Societa' Italiana di Cardiologia; SIC) (G.V.).

Received for publication Dec 14, 2011; final revision accepted Apr 13, 2012

Reprint requests: Thomas H. Schindler, MD, Division of Cardiology, Nuclear Cardiology and Cardiac PET/CT, Department of Specialities in Medicine, University Hospital of Geneva, 6th Floor, Rue Gabrielle-Perret-Gentil 4, 1211 Geneva, Switzerland; *thomas.schindler@hcuge.ch*.

1071-3581/$34.00

doi:10.1007/s12350-012-9570-5

demonstrated to provide substantial diagnostic and prognostic information additional to that derived from angiographic and coronary risk factor assessment.[1-6] The exact pathophysiological mechanisms underlying abnormal coronary circulatory function remain to be further elucidated, but increases in reactive oxygen species associated with an inflammation of the arterial wall have been suggested as a common final pathway of a variability of cardiovascular risk factors to alter the coronary vasodilator capacity.[7-9] In the normal setting, coronary flow increases for maintaining an appropriate metabolic and oxygen supply of the left ventricle adapt according to its inotropic state at rest or during physiological stress.[10-13] This relationship between left-ventricular function and myocardial flow is also referred to as myocardial perfusion-contracting matching.[14] Toward this direction, myocardial tagging techniques with MRI have provided new insight into normal and abnormal patterns of regional cardiac contractility.[15,16] Previous investigations[16] have provided some first evidence that a diminished myocardial flow reserve (MFR) may be paralleled by a reduced regional myocardial function in asymptomatic cardiovascular risk individuals as determined with contrast-enhanced MRI perfusion and tagging studies. As we and others have demonstrated,[17-19] increases in body weight are commonly paralleled by a progressive dysfunction of the coronary circulation, while it may also alter regional LV function in obese individuals.[20] The possible relationship between coronary circulatory function and corresponding regional contractility in healthy, normal-weight, and those with increasing body weight, however, remains to be elucidated.

With this in mind, we aimed to define a possible relationship between regional coronary vasodilator capacity and myocardial circumferential strain or wall motion at rest in normal-weight, overweight, and obese individuals with normal global left-ventricular function.

METHODS

Study Population and Design

The study population included 32 asymptomatic individuals without traditional cardiovascular risk factors such as arterial hypertension, hypercholesterolemia, smoking, and diabetes mellitus (Table 1). Study participants underwent an initial screening visit that included a physical examination, electrocardiogram (ECG), blood pressure measurements, and routine blood chemistry in a fasting state. Excluded were study candidates with a history of variant angina, a family history of premature CAD, or clinically manifest cardiovascular or any other disease. In addition, no study participant was on any cardiac or vasoactive medication. Physical examination revealed normal findings in all study participants and they had normal resting ECGs. All study participants then underwent ^{13}N-ammonia PET/CT (64-slice Biograph HiRez TruePoint PET-CT scanner, Siemens, Erlangen, Germany) measurements of myocardial blood flow (MBF) at rest and

Table 1. Characteristics of study population (n = 32)

	CON (n = 12)	OW (n = 10)	OB (n = 10)	*P* value
Age (years)	49 ± 17	44 ± 13	48 ± 6	.535
Gender, F/M	6/8	4/6	4/6	/
BMI (kg/m^2)	22.7 ± 2.82	27.8 ± 1.52	38.4 ± 5.35	.0001
Waist-hip ratio	0.81 ± 0.08	0.87 ± 0.06	0.94 ± 0.04	.0001
Waist (cm)	83.3 ± 8.39	97.6 ± 8.11	117.6 ± 9.94	.0001
Hip (cm)	102.7 ± 4.64	111.8 ± 4.30	124.5 ± 9.07	.0001
Laboratory result				
Cholesterol levels (mg/dL)	186.7 ± 41.90	208.2 ± 35.16	194.7 ± 40.06	.366
LDL level (mg/dL)	130.0 ± 17.98	147.3 ± 16.71	128.2 ± 29.49	.094
HDL level (mg/dL)	48.2 ± 12.11	44.6 ± 14.33	43.8 ± 15.22	.720
Triglyceride level (mg/dL)	80.5 ± 33.46	114.8 ± 49.11	117.5 ± 46.02	.056
Glucose level (mg/dL)	96.3 ± 7.95	95.2 ± 8.16	96.5 ± 7.61	.894
Insulin (mUI/L)	3.0 ± 1.77	12.8 ± 9.31	12.8 ± 6.44	.0001
HOMA	0.70 ± 0.51	2.62 ± 1.68	2.96 ± 1.27	.0001
hs-CRP levels (mg/L)	1.77 ± 1.46	2.66 ± 3.31	7.03 ± 5.58	.008
HbA_{Ic} (%)	5.26 ± 0.18	5.36 ± 0.31	5.34 ± 0.30	.397

Values are mean ± SD.
P values between groups by ANOVA.
CON, Controls; *OW*, overweight; *OB*, obesity; *BMI*, body mass index; *hs-CRP*, high sensitive C-reactive protein; *HbA_{Ic}*, hemoglobin A_{Ic}; *HDL*, high-density lipoprotein; *HOMA*, homeostasis model assessment; *LDL*, low-density lipoprotein.

during pharmacologically induced hyperemia with dipyridamole in a fasting state to evaluate coronary circulatory function. A prerequisite for the study inclusion was a normal stress-rest perfusion imaging on ^{13}N-ammonia PET/CT, which widely excluded the presence of flow-limiting epicardial CAD lesions.[18] Following, study participants were grouped according to their body mass index (BMI, kg/m^2): control group $20 \leq$ BMI < 25 (CON; n = 12), overweight group $25 \leq$ BMI $<$ 30 (OW; n = 10), obese group BMI ≥ 30 (OB; n = 10).

Blood chemistry included plasma glucose, hemoglobin A1c, insulin, total cholesterol, HDL and LDL cholesterol, triglycerides levels, and high-sensitive C-reactive protein. In addition, Homeostasis Model Assessment (HOMA) was calculated as index of insulin resistance (HOMA = fasting plasma glucose [mmol/L] × fasting plasma insulin [pmol/L]/162).[21] Within 20 days of the cardiac ^{13}N-ammonia PET/CT study, cardiac magnetic resonance (CMR) tagging was performed using a 1.5T Espree system (Siemens Medical Solutions, Erlangen, Germany) to evaluate possible alterations in global and regional myocardial motion patterns.[22] The study was approved by the University Hospitals of Geneva Institutional Review Board (No: 07-183), and each participant signed the approved informed consent form.

Quantification of MBF with PET/CT

Following the topogram used to define the axial field-of-view and a low-dose CT scan (120 kV, 30 mA) for attenuation correction, PET emission data were acquired during shallow breathing following intravenous injection of ≈500-550 MBq of ^{13}N-ammonia. The CT-based attenuation correction map was used to reconstruct the PET emission data. MBF quantification was performed first at rest and then during pharmacologic vasodilation with dipyridamole-induced hyperemia applying intravenously standard dose of 140 μg/kg/minute.[23,24] The relative distribution of ^{13}N-ammonia uptake of the left ventricle was assessed visually on short- and long-axis myocardial slices and semiquantitatively on the corresponding polar map from the last static 18-minute transaxial PET image. Time-activity curves from the first 12-dynamic frames (12 for 10 seconds each), in concert with a two-compartment tracer kinetic model,[25] were used to calculate global and regional MBF in mL/g/minute of the left ventricle with the use of the PMOD software package (version 2.8 PMOD Technologies Ltd, Zurich, Switzerland).[18] Regional MBFs of the LAD, LCx, and RCA territory were averaged on a polar map and the resulting mean MBF was defined as global MBF of the left ventricle. Heart rate, blood pressure, and a 12-lead ECG were recorded continuously during each MBF measurement. From the average of heart rate and blood pressure during the first 2 minutes of each image acquisition, the rate-pressure product (RPP) was determined as an index of cardiac work. To account for interindividual variations in coronary driving pressure, an index of coronary vascular resistance (CVR) was determined as the ratio of mean arterial blood pressure to MBF (mm Hg/mL/minute/g).

Protocol for Tagged MRI

Image acquisition. Study participants underwent MRI examination using a 1.5T Espree system (Siemens Medical Solutions, Erlangen, Germany). Individuals were scanned in the supine position, using a 6-element anterior body array coil combined with a 6-element posterior spine coil. Following the acquisition of localizers, 2-chamber, 4-chamber, and short axis high-resolution steady state free precession (SSFP) cine imaging (pixel size = 1.3 × 1.3 × 7 mm^3, temporal resolution ≈ 25-40 ms), myocardial tagging was performed in a three short axis view with complementary spatial modulation of magnetization technique.[26] We used a prospectively ECG-gated, balanced SSFP.[22] The field of view was 340 × 340 mm, matrix 192 with 32% phase resolution, slice thickness 7 mm, TE 1.2, and flip angle 20°. Tag distance was 7 mm and localized shimming to adjust the static magnetic field within each slice was performed prior to acquisition. The temporal resolution was 25-40 ms, depending on the heart rate and breath-hold capacity of the subjects. The two tag line directions were acquired in a single breath-hold in end-expirium.

Strain analysis. For tag analysis, we used extrema temporal chaining.[27] Strain analysis describes the change of shape of material (i.e., myocardium) resulting from deformation, which are used to present regional myocardial function.[26] In this study, maximal circumferential strain (ϵc, %), reflecting intramural circumferential shortening and defined as ϵc = length (time t) − length (time 0)/(time 0),[26] was calculated semi-automatically from the tracked points of the mid-wall in six cardiac sectors for three slices (3 short axis views). Length is given in millimeter and time in seconds. The sectors were defined according to the AHA 17-segment model.[28] Further, the sectors were defined by the software starting from the RV/LV border assigned by the user. For this study, we focused on the mid-wall systolic circumferential shortening, using timing information (onset and peak time) and the mid-wall systolic circumferential strain. When mentioned, ''wall motion,'' it refers to max-min of the circumferential shortening time curve in the considered cardiac sector. The circumferential strain data were averaged in the three main coronary perfusion territories according subtended to the LAD, LCx, and RCA. The global systolic circumferential strain (gϵc) was defined as the circumferential strain averaged across all segments.[16] Further, obesity is commonly associated with elevations in arterial blood pressures and, thus, myocardial workload,[18] leading to an increase in left ventricular preload, which may alter global and regional circumferential strain. ϵc, therefore, was normalized to the RPP at rest (Nϵc = ϵc divided by RPP rest multiplied by 10000) to compensate for possible interindividual variations in ϵc (%) due to hemodynamic differences.

Statistical Analysis

Data are presented as mean ± SD for quantitative and absolute frequencies for qualitative variables. The appropriate Wilcoxon rank test for independent or paired samples was used. Comparison between the different groups was performed by one-way analysis of variance, followed by Scheffe's multiple

comparison tests. Pearson's correlation coefficient (r), assuming a linear regression, was calculated to investigate possible associations between MBF and CVR, myocardial strain, and hemodynamic parameters. Statistical significance was assumed if a null hypothesis could be rejected at $P = .05$. All statistical analyses were performed with SPSS for Windows 18.0 (SPSS).

RESULTS

Patient Characteristics

The clinical and metabolic profiles among the three groups studied are given in Table 1. The increase in BMI and waist-hip ratio in the three study groups was accompanied by a significant increase in fasting insulin plasma levels, HOMA as index for insulin resistance, triglycerides, and hs-CRP plasma levels. Conversely, lipid profile, glucose plasma levels, and HbA1c did not differ significantly between groups.

Hemodynamics and Global MBF

At baseline, heart rate was comparable between CON and OW, while it was higher in OB (Table 2). Further, SBP and DBP did not differ significantly between groups. As heart rate was higher in OB, also the resting RPP was significantly higher in OB than in CON and OW. As regards, the resting MBF was higher in OB but not significantly different among groups. During dipyridamole stimulation of hyperemic flows, heart rates increased significantly from rest, but they were comparable among groups (Table 2). In addition, SBP mildly decreased during dipyridamole stimulation from rest in CON and OB, while it remained largely unchanged in OW. There were no significant differences in heart rate during pharmacologic vasodilation among the study groups. Conversely, SBP, DBP, and the RPP progressively increased from CON to OW and OB during dipyridamole stimulation (Table 2).

Compared with CON, global hyperemic MBFs and MFR tended to be lower in OW but they decreased significantly in OB (Figure 1; Table 2). When the global hyperemic MBFs were related to the mean arterial blood pressure to account for possible interindividual variations in coronary driving pressure, the global CVR (mean arterial blood pressure/MBF) widely mirrored the MBF values during pharmacologic vasodilation for each

Table 2. Global circumferential strain derived from tagging MRI and global myocardial blood flow (gMBF), coronary vascular resistance (gCVR), and hemodynamic findings during PET/CT exam

	Groups			
	CON	**OW**	**OB**	***P* value**
ϵ_c (%)	−0.24 ± 0.03	−0.23 ± 0.02	−0.23 ± 0.04	.918
Nϵ_c (%)	−0.31 ± 0.06	−0.32 ± 0.05	−0.26 ± 0.08	.096
gMBF (mL/minute/g)				
gMBF at rest	0.78 ± 0.15	0.74 ± 0.18	0.85 ± 0.23	.382
gMBF during hyperemia	2.21 ± 0.47	1.94 ± 0.49	1.50 ± 0.41	.006
gMFR	2.98 ± 0.96	2.70 ± 0.66	1.98 ± 1.04	.052
gCVR (mm Hg/mL/minute/g)				
At rest	110.8 ± 19.70	119.2 ± 29.64	113.2 ± 28.71	.745
Pharmacologic vasodilation	36.6 ± 10.11	47.8 ± 14.88	60.6 ± 13.62	.001
Hemodynamics at rest				
Heart rate (beats/minute)	63.6 ± 4.21	62.5 ± 8.19	74.3 ± 14.7	.018
SBP (mm Hg)	115 ± 10.87	116.7 ± 10.3	122.3 ± 9.57	.251
DBP (mm Hg)	68.8 ± 9.58	66.9 ± 7.81	75.3 ± 8.22	.089
RPP	7318 ± 921	7247 ± 803	9151 ± 2378	.011
Pharmacologic vasodilation				
Heart rate (beats/minute)	83.1 ± 7.25	86.2 ± 5.98	89.8 ± 34.42	.738
SBP (mm Hg)	110.3 ± 9.96	117.4 ± 9.32	121.3 ± 12.28	.059
DBP (mm Hg)	60.3 ± 6.59	64.3 ± 7.41	69.5 ± 10.69	.048
RPP	9125 ± 817	10140 ± 1282	11878 ± 2257	.001

Values are mean ± SD.
P values between groups by ANOVA.
CON, Controls; *OW*, overweight; *OB*, obesity; ϵ_c (%), maximal circumferential strain; Nϵ_c (%), normalized ϵ_c (%); *MBF*, myocardial blood flow; *MFR*, myocardial flow reserve; *CVR*, coronary vascular resistance; *SBP*, systolic blood pressure.

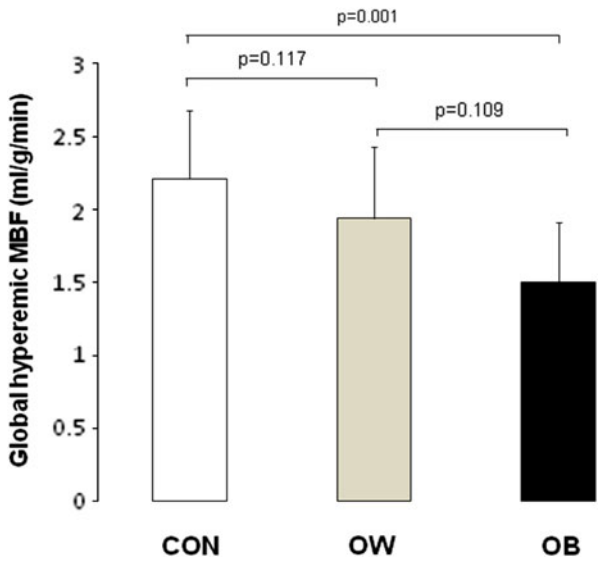

Figure 1. Global hyperemic MBF in CON, OW, and OB.

group studied (Table 2). The group comparison of global hyperemic MBF, CVR, and MFR in CON was significantly different from OW and OB, respectively ($P \leq .05$ by ANOVA).

Regional MBFs and Circumferential Strain

Regional MBFs at rest, during pharmacologically induced hyperemia and the corresponding MFR in the territory supplied by the LAD, LCx, and RCA did not differ significantly within CON, OW, and OB (Table 3). The intergroup comparison did not reveal significant differences among groups for regional resting flow, whereas regional hyperemic MBF and MFR were significantly lower in OB. In addition, regional CVR at rest and during dipyridamole stimulation widely mirrored those of regional MBF of study group (Table 3). As regards, the maximal circumferential strain (Ɛc,%), global Ɛc (gƐc,%), for all segments was -0.23 ± 0.03 and it did not differ significantly between groups (Table 2; Figure 2). Also, the normalized gƐc (gNƐc) was comparable between CON and OW, while significantly lower in OB ($P = .006$ and $P = .012$, respectively) (Table 2). Addressing regional Ɛc and NƐc within each group (Table 3), they were significantly greater in the LCx than in the LAD and lower in the RCA territory ($P < .05$). While regional Ɛc for the LAD, LCX, and RCA territory did not differ between groups, the corresponding NƐc values in OB were significantly lower to those in CON and in OW.

Table 3. Regional MBF, CVR, and circumferential strain

	CON			OW			OB		
	LAD	LCx	RCA	LAD	LCx	RCA	LAD	LCx	RCA
MBF rest	0.78 ± 0.18	0.81 ± 0.19	0.75 ± 0.12	0.73 ± 0.16	0.75 ± 0.20	0.74 ± 0.22	0.86 ± 0.23	0.85 ± 0.27	0.86 ± 0.23
CVR rest	111 ± 221	106 ± 22	112 ± 18	119 ± 28	118 ± 30	121 ± 37	111 ± 29	117 ± 42	110 ± 24
MBF hyperemia	2.08 ± 0.54	2.30 ± 0.54	2.16 ± 0.56	1.82 ± 0.51	1.96 ± 0.55	1.83 ± 0.55	1.50 ± 0.40	1.50 ± 0.39	1.49 ± 0.47*
CVR hyperemia	39 ± 11	36 ± 13	38 ± 14	49 ± 16	46 ± 14	49 ± 17	61 ± 15	61 ± 13	62 ± 15*
MFR	2.83 ± 1.04	2.99 ± 1.08	2.94 ± 0.98	2.54 ± 0.72	2.72 ± 0.81	2.59 ± 0.85	1.96 ± 1.07	2.06 ± 1.24	1.89 ± 0.95*
Ɛc (%)	−0.23 ± 0.03	−0.26 ± 0.04	−0.21 ± 0.05	−0.22 ± 0.02	−0.26 ± 0.03	−0.21 ± 0.03	−0.22 ± 0.05	−0.27 ± 0.06	−0.21 ± 0.03
NƐc (%)	−0.33 ± 0.08	−0.36 ± 0.06	−0.29 ± 0.08	−0.31 ± 0.06	−0.35 ± 0.05	−0.29 ± 0.06	−0.25 ± 0.08	−0.31 ± 0.09	−0.24 ± 0.06*

MBF, Myocardial blood flow (mL/g/minute); *CVR*, coronary vascular resistance (mm Hg/mL/g/minute); *MFR*, myocardial flow reserve; *DP*, dipyridamole; Ɛc (%), maximal circumferential strain; *N*Ɛc (%), normalized Ɛc.
* $P \leq .05$ between groups by ANOVA.

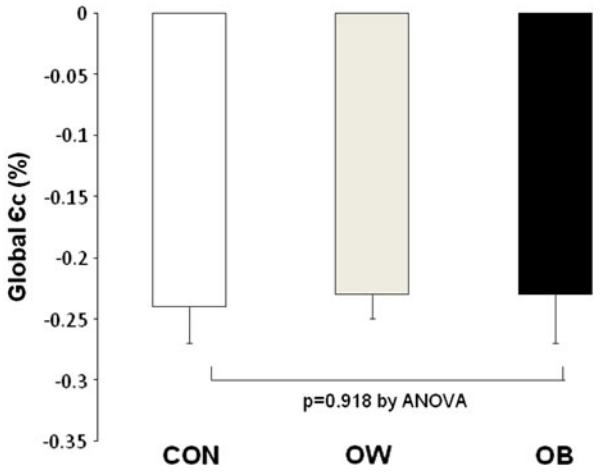

Figure 2. Global maximal circumferential strain (Ɛc, %) at rest in CON, OW, and OB.

Relation Between MBFs, Hemodynamics, and Circumferential Strain

For the whole study population, global resting MBF significantly correlated with the corresponding RPP ($r = 0.57$, $P < .001$, SEE = 0.16). Conversely, there was no association between global hyperemic MBFs during pharmacologic vasodilation, MFR, and corresponding RPP, respectively ($r = -0.23$, $P = .188$, SEE = 0.54 and $r = 0.25$, $P = .174$, SEE = 0.97). As regards global Ɛc and NƐc, they correlated inversely with resting RPP, respectively ($r = -0.32$, $P = .057$, SEE = 0.03 and $r = -0.82$, $P < .0001$, SEE = 967). In addition, when evaluating the relationship between global Ɛc and global MBF at rest, during hyperemia, and MFR, respectively, no association was observed ($r = -0.26$, $P = .144$, SEE = 0.185; $r = 0.30$, $P = .096$, SEE = 0.527; and $r = 0.32$, $P = .071$, SEE = 0.947). In contrast to this, global NƐc correlated significantly and inversely with global resting MBF ($r = -0.52$, $P = .002$, SEE = 0.164), while positively with global hyperemic MBF and MFR, respectively ($r = 0.55$, $P = .001$, SEE = 0.462 and $r = 0.64$, $P < .0001$, SEE = 0.765).

Regarding regional Ɛc, no relationship with regional MBF or with corresponding CVR at rest in CON, OW, and OB was observed (Table 4). Conversely, regional Ɛc and corresponding hyperemic MBF, CVR, and MFR correlated in CON and OW but not in OB (Figure 3). Further, we evaluated possible associations between normalized regional Ɛc (NƐc) and coronary flow parameters (Table 4). As it was observed, regional NƐc did not correlate with corresponding MBF at rest in CON and OW, while there was a significant and inverse association in OB. Interestingly, when regional NƐc was related to the CVR at rest, it correlated in OW and OB but not in CON. Further, regional NƐc was significantly associated with hyperemic MBF and MFR in CON and OW, but again not in OB. However, when possible interindividual differences in intracoronary driving pressure were

Table 4. Correlations between regional maximal circumferential strain and flow parameters

	CON		OW		OB	
	Ɛc (%)	**NƐc (%)**	**Ɛc (%)**	**NƐc (%)**	**Ɛc (%)**	**NƐc (%)**
MBF rest	$r = 0.07$	$r = 0.16$	$r = 0.02$	$r = -0.29$	$r = -0.25$	**$r = -0.51$**
	$P = .712$	$P = .340$	$P = .906$	$P = .120$	$P = .178$	**$P = .004$**
	SEE = 0.16	SEE = 0.16	SEE = 0.66	SEE = 0.18	SEE = 0.23	**SEE = 0.21**
MBF hyperemia	**$r = 0.42$**	**$r = 0.64$**	**$r = 0.47$**	**$r = 0.37$**	$r = 0.09$	$r = 0.23$
	$P = .011$	**$P < .0001$**	**$P = .006$**	**$P = .046$**	$P = .636$	$P = .220$
	SEE = 0.49	**SEE = 0.40**	**SEE = 0.47**	**SEE = 0.51**	SEE = 0.43	SEE = 0.41
MFR	**$r = 0.36$**	**$r = 0.58$**	**$r = 0.54$**	**$r = 0.63$**	$r = 0.03$	$r = 0.30$
	$P = .030$	**$P < .0001$**	**$P = .002$**	**$P < .0001$**	$P = .880$	$P = .120$
	SEE = 0.95	**SEE = 0.81**	**SEE = 0.66**	**SEE = 0.62**	SEE = 1.07	SEE = 0.90
CVR rest	$r = 0.20$	$r = 0.02$	$r = 0.12$	**$r = 0.37$**	$r = 0.14$	**$r = 0.37$**
	$P = .237$	$P = .892$	$P = .525$	**$P = .046$**	$P = .472$	**$P = .043$**
	SEE = 19.8	SEE = 20.2	SEE = 31.4	**SEE = 29.4**	SEE = 31.6	**SEE = 29.6**
CVR hyperemia	**$r = -0.42$**	**$r = -0.70$**	**$r = -0.54$**	**$r = -0.34$**	$r = -0.16$	**$r = -0.46$**
	$P = .011$	**$P < .0001$**	**$P = .002$**	**$P = .056$**	$P = .409$	**$P = .010$**
	SEE = 11.2	**SEE = 8.79**	**SEE = 13.3**	**SEE = 14.8**	SEE = 15.1	**SEE = 12.6**

Significant correlations are indicated in bold.
MBF, Myocardial blood flow (mL/g/minute); *MFR*, myocardial flow reserve; *CVR*, coronary vascular resistance (mm Hg/mL/g/minute); Ɛc (%), maximal circumferential strain; *NƐc* (%), normalized Ɛc; *SEE*, standard error of the estimate.

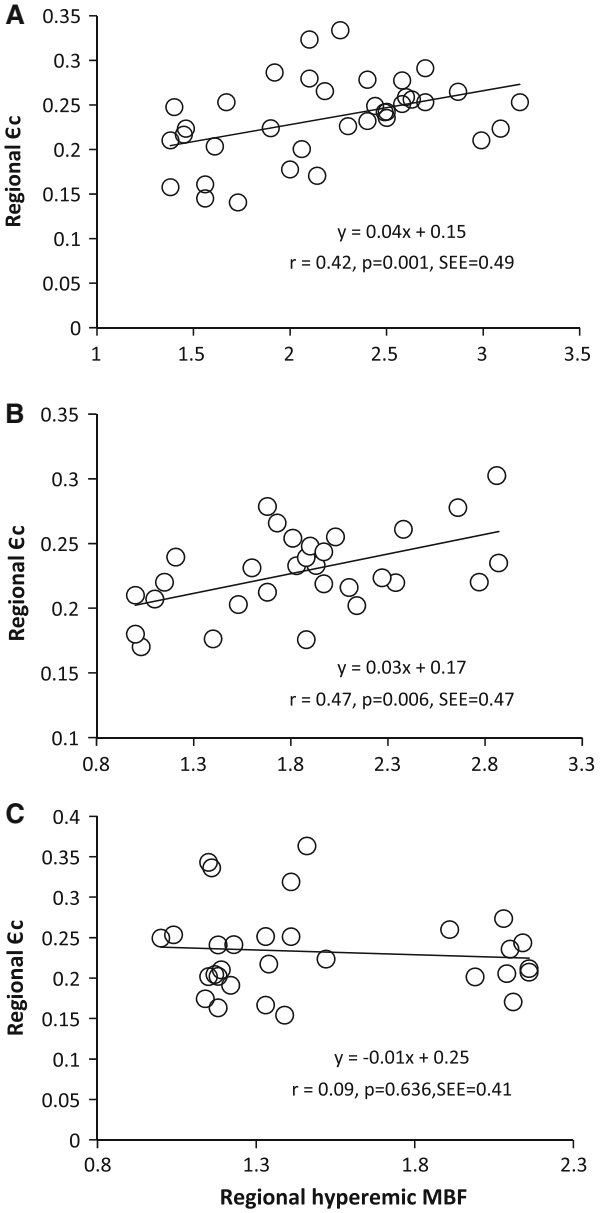

Figure 3. Correlation between regional hyperemic MBF in the territory subtended to the LAD, LCx, and RCA and corresponding local €c at rest (%, positive values for display) in CON (**A**), OW (**B**), and OB (**C**).

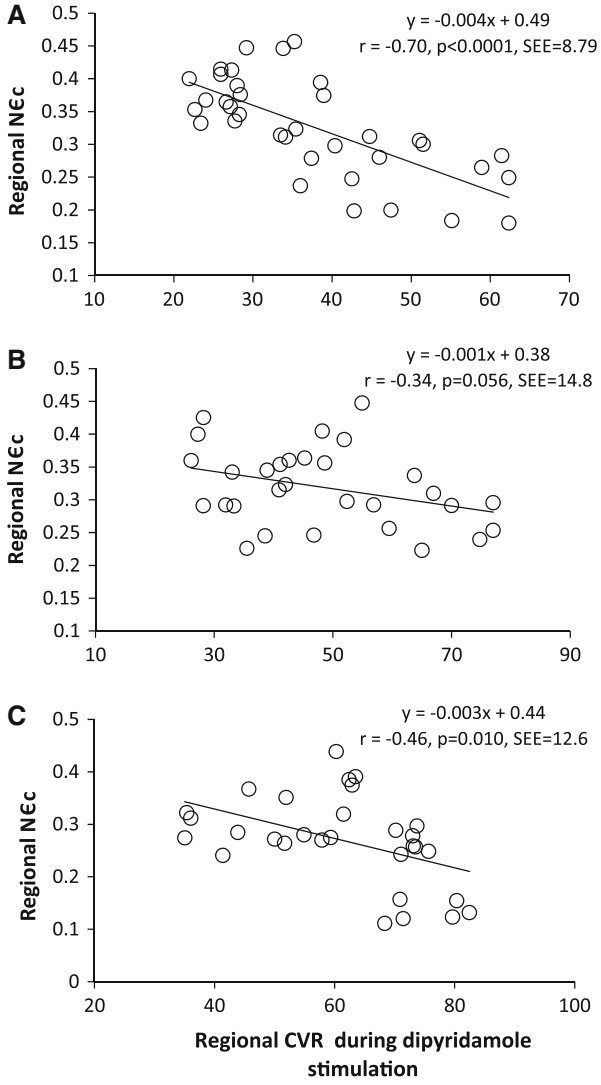

Figure 4. Correlation between regional CVR during dipyridamole stimulation in the territory subtended to the LAD, LCx, and RCA and corresponding local N€c at rest (%, positive values for display) in CON (**A**), OW (**B**), and OB (**C**).

accounted by the calculated regional CVR, there was a significant and inverse relationship between regional N€c and corresponding CVR during dipyridamole stimulation in all the three groups (Figure 4, Table 4).

DISCUSSION

This study is unique in demonstrating a positive association between increases in regional hyperemic MBFs or MFR as determined with ^{13}N-ammonia PET and corresponding regional resting circumferential strain as assessed with tagging MRI in healthy non-obese individuals. Regional increases of coronary vasodilator function, therefore, were paralleled by an enhanced local circumferential strain at rest. This relationship was also observed for obese individuals with reduced hyperemic MBFs but only when values of circumferential strain were normalized to the RPP and related to the CVR during dipyridamole stimulation. When looking at the obesity group with a marked impairment of hyperemic MBFs and MFR, regional coronary vasodilator function at first sight was not correlated with resting circumferential strain. The reason for this observation appears to be related to confounding effects of higher heart rates,

SBPs, and resulting RPP, indicative of the myocardial workload, not only at rest but also at pharmacologic stress in OB when compared to CON and OW. In order to account for this confounding hemodynamic factor, which may lead to interindividual differences in coronary driving pressure and an increase in left ventricular preload or extra-vascular resistive forces, regional CVR and normalized circumferential strain (Nϵc) were also evaluated. And indeed, when regional resting Nϵc was related to corresponding CVR during pharmacologic vasodilation, we observed a significant and inverse association. Thus, the higher regional resting Nϵc was associated with a relatively lower regional CVR during pharmacologic vasodilation in OB. To our best knowledge, these findings are first to suggest a conditioning of the coronary vasodilator capacity by resting regional circumferential strain in healthy individuals with increasing body weight, which deserves further investigations.

Resting MBFs, RPP, and Circumferential Strain

As observed in the current and previous investigations,[10,12] there is a close linear association between resting MBF and the RPP as an index of cardiac work and thus myocardial oxygen demand. Increases in myocardial work, therefore, are closely paralleled by commensurate MBF increases to appropriately meet increases in oxygen demand. Interestingly, we could also demonstrate an inverse association between global ϵc and resting RPP. Increases in resting RPP, therefore, were associated with relatively lower global circumferential strain, which can be related to the dependency of regional myocardial function on left ventricular preload and afterload, and thus on hemodynamic conditions.[16] Such observation could also explain why global ϵc did not correlate with corresponding resting MBF, whereas a significant and inverse association was observed for global Nϵc. Taken together, however, these unique observations denote a close interrelation between the regulation of resting MBF, myocardial work load, and circumferential strain.[14]

In agreement with recent investigation,[18] resting MBFs in OB was higher than in CON and in OW. This relative increase in resting global MBF in OB can be related to higher resting heart rates, SBPs, and corresponding RPP and, in turn, myocardial oxygen consumption.[10] The finding of an increase in myocardial workload in OB paralleled by higher resting MBF also accords with previously reported activation of the sympathetic nervous system and renin-angiotensin-aldosterone system.[18,29] Notably, an increase in arterial blood pressure at rest may have led not only to an elevation in resting myocardial workload and, thus, MBF but also to increase in left ventricular preload and extra-vascular resistive forces, which, in turn, may have affected the global circumferential strain. And indeed, when we compensated for differences in hemodynamic effects due to increases in resting RPP by calculating the Nϵc, the global and regional Nϵc was lower in OB, while comparable between CON and OW. Of further interest, when we related regional resting Nϵc to corresponding regional CVR, we observed a positive and significant association in OW and in OB but not in CON. This observation may stress that in individuals with increasing body weight and an increase in left ventricular preload and extra-vascular resistive forces, left ventricular myocardium underlies an adaptive and relative increase regional Nϵc aiming to maintain the left ventricular ejection volume, which is also known to reflect the Frank-Starling mechanism.[30,31] This, in fact, could signify a conditioning of the resting coronary flow by an adaptive increase in regional circumferential wall motion in individuals with increasing body weight. Conversely, in the more recently reported multi-ethnic study of atherosclerosis (MESA) trial, conducted in 74 asymptomatic cardiovascular risk individuals,[16] and also in the 12 CON of this study, resting regional MBF and corresponding circumferential strain did not closely accompany each other. Thus, it appears that with increases in left ventricular pre-load due to relative elevations in arterial blood pressures, as observed in individuals with increasing body weight, an adaptive increase in regional circumferential wall motion ensues associated with a commensurate change in resting MBF.

Coronary Vasodilator Capacity and Circumferential Strain

As regards, global hyperemic MBFs and MFR were observed to be non-significantly lower in OW when compared to CON, while declining significantly in OB. This accords with previous reports,[17,18,29] emphasizing some adverse effects of increasing body weight on the coronary vasodilator capacity. In the aforementioned MESA trial,[16] myocardial flow and myocardial circumferential strain were assessed with cardiac MRI and evaluated in asymptomatic individuals but with various traditional cardiovascular risk factors such as arterial hypertension, hypercholesterolemia, smoking, and diabetes mellitus. It was observed that the coronary vasodilator capacity correlated inversely with myocardial circumferential strain.[16] Accordingly, in the MESA trial diminished hyperemic flows were paralleled by reduced resting circumferential strain in cardiovascular risk individuals.[16] Therefore, not only the regional coronary vasodilator capacity but also the corresponding

circumferential strain was altered by classical cardiovascular risk factors in asymptomatic and relatively old individuals with a mean age of 65 years. The underlying mechanisms remain uncertain but one possibility is that classical cardiovascular risk factors have led, at least in part, to increases of reactive oxygen species and micro-inflammation in the arterial wall with reductions in the bioavailability of endothelium-derived nitric oxide as a common final pathway underlying coronary vasodilator dysfunction and, possibly, also leading to regional myocardial dysfunction.[32,33] With this study, however, we extend the observation of an association between regional coronary vasodilator capacity and corresponding resting myocardial circumferential strain to healthy individuals with increasing body weight but without traditional cardiovascular risk factors. This may argue in favor of yet unknown physiological mechanisms or interactions between regional coronary vasodilator capacity and resting circumferential strain. Under physiologic circumstances, cardiac function determines myocardial oxygen consumption and consequently coronary perfusion.[6,14] On the other hand, there is also experimental evidence that an increase in coronary perfusion is related to an elevation in oxygen consumption and contractile function, the so called Gregg phenomenon.[34] This phenomenon is likely secondary to enhanced diastolic distension due to filling of the coronary microcirculation, also named ''garden house effect,'' which may support our observations. Someone could also argue that, within the complexity of myocardial perfusion-contraction matching,[14,35] an increase in regional circumferential strain at rest is also a reflection of increase in the demand for hyperemic MBFs or MFR, respectively, to maintain an appropriate metabolic and oxygen supply. The described relationship between regional coronary vasodilator capacity and corresponding resting circumferential strain, however, may also put forth a conditioning of the coronary vasodilator capacity by resting regional myocardial circumferential strain. While such a novel concept may be intuitively correct, it awaits further confirmation by well-elaborated experimental and clinical investigations.

LIMITATIONS

There are some limitations worthy of consideration in interpreting these data. First, diffuse CAD and/or focal structural alterations of the arterial wall could have mildly affected hyperemic MBFs.[24,36] As normal stress and rest myocardial perfusion images with ^{13}N-ammonia and PET/CT was an inclusion criterion for study participants, effects of flow-limiting epicardial lesions can be widely ruled out.[1] In addition, because study participants were asymptomatic, the performance of non-invasive MDCT coronary angiography[37] to visualize coronary morphology and structure did not seem to be justified. For this reason, some subclinical structural CAD with mild downstream effects on coronary flows may have been missed in this study population.[24,36,38] Second, it may be seen as a limitation that, apart from the left ventricular circumferential strain at rest, we did not measure peak longitudinal strain with tagging MRI due to time constraints, which might have been more sensitive in the identification of subtle abnormalities of regional LV contractile function.[20,39] Although, measures of circumferential strain with cardiac MRI are of high precision due to numerous tags around the perimeter of the heart,[26] which yields a high sensitivity in the identification of subtle regional myocardial motion abnormalities,[40] information on the reproducibility of strain measurements is still lacking. Also, the assessment of regional circumferential strain with cardiac MRI during dobutamine stimulation would have been a better approach to depict a possible perfusion-contraction mismatch in OB individuals during times demand-induced flow supply,[41,42] which should be evaluated in future studies. Finally, in view of the relatively low number of study participants, current findings may rather be seen as exploratory, while they are likely to stimulate further clinical investigations in this developing research field.

CONCLUSIONS

Higher coronary vasodilator capacity is related to corresponding regional circumferential strain at rest in non-obese individuals, while this is also observed for reduced hyperemic flows and MFR in obesity.

Conflict of interest

No potential conflict of interest exists.

References

1. Schindler TH, Schelbert HR, Quercioli A, Dilsizian V. Cardiac PET imaging for the detection and monitoring of coronary artery disease and microvascular health. JACC Cardiovasc Imaging 2010;3:623-40.
2. Lerman A, Zeiher AM. Endothelial function: Cardiac events. Circulation 2005;111:363-8.
3. Schindler TH, Nitzsche EU, Schelbert HR, Olschewski M, Sayre J, Mix M, et al. Positron emission tomography-measured abnormal responses of myocardial blood flow to sympathetic stimulation are associated with the risk of developing cardiovascular events. J Am Coll Cardiol 2005;45:1505-12.
4. Ziadi MC, Dekemp RA, Williams KA, Guo A, Chow BJ, Renaud JM, et al. Impaired myocardial flow reserve on rubidium-82 positron emission tomography imaging predicts adverse outcomes in patients assessed for myocardial ischemia. J Am Coll Cardiol 2011;58:740-8.

5. Herzog BA, Husmann L, Valenta I, Gaemperli O, Siegrist PT, Tay FM, et al. Long-term prognostic value of 13N-ammonia myocardial perfusion positron emission tomography added value of coronary flow reserve. J Am Coll Cardiol 2009;54:150-6.
6. Schindler TH, Zhang XL, Mhiri L, Lerch R, Schelbert HR. Role of PET in the evaluation and understanding of coronary physiology. J Nucl Cardiol 2007;14:589-603.
7. Munzel T, Gori T, Bruno RM, Taddei S. Is oxidative stress a therapeutic target in cardiovascular disease? Eur Heart J 2010;31:2741-8.
8. Schindler TH, Nitzsche EU, Olschewski M, Magosaki N, Mix M, Prior JO, et al. Chronic inflammation and impaired coronary vasoreactivity in patients with coronary risk factors. Circulation 2004;110:1069-75.
9. Vaccarino V, Khan D, Votaw J, Faber T, Veledar E, Jones DP, et al. Inflammation is related to coronary flow reserve detected by positron emission tomography in asymptomatic male twins. J Am Coll Cardiol 2010;57:1271-9.
10. Czernin J, Barnard RJ, Sun KT, Krivokapich J, Nitzsche E, Dorsey D, et al. Effect of short-term cardiovascular conditioning and low-fat diet on myocardial blood flow and flow reserve. Circulation 1995;92:197-204.
11. Krivokapich J, Czernin J, Schelbert HR. Dobutamine positron emission tomography: Absolute quantitation of rest and dobutamine myocardial blood flow and correlation with cardiac work and percent diameter stenosis in patients with and without coronary artery disease. J Am Coll Cardiol 1996;28:565-72.
12. Chareonthaitawee P, Kaufmann PA, Rimoldi O, Camici PG. Heterogeneity of resting and hyperemic myocardial blood flow in healthy humans. Cardiovasc Res 2001;50:151-61.
13. Schelbert HR. Anatomy and physiology of coronary blood flow. J Nucl Cardiol 2010;17:545-54.
14. Heusch G, Schulz R. Perfusion-contraction match and mismatch. Basic Res Cardiol 2001;96:1-10.
15. Garot J, Bluemke DA, Osman NF, Rochitte CE, McVeigh ER, Zerhouni EA, et al. Fast determination of regional myocardial strain fields from tagged cardiac images using harmonic phase MRI. Circulation 2000;101:981-8.
16. Rosen BD, Lima JA, Nasir K, Edvardsen T, Folsom AR, Lai S, et al. Lower myocardial perfusion reserve is associated with decreased regional left ventricular function in asymptomatic participants of the multi-ethnic study of atherosclerosis. Circulation 2006;114:289-97.
17. Schindler TH, Cardenas J, Prior JO, Facta AD, Kreissl MC, Zhang XL, et al. Relationship between increasing body weight, insulin resistance, inflammation, adipocytokine leptin, and coronary circulatory function. J Am Coll Cardiol 2006;47:1188-95.
18. Quercioli A, Pataky Z, Vincenti G, Makoundou V, Di Marzo V, Montecucco F, et al. Elevated endocannabinoid plasma levels are associated with coronary circulatory dysfunction in obesity. Eur Heart J 2011;32:1369-78.
19. Al Suwaidi J, Higano ST, Holmes DR Jr, Lennon R, Lerman A. Obesity is independently associated with coronary endothelial dysfunction in patients with normal or mildly diseased coronary arteries. J Am Coll Cardiol 2001;37:1523-8.
20. Vinereanu D, Madler CF, Gherghinescu C, Ciobanu AO, Fraser AG. Cumulative impact of cardiovascular risk factors on regional left ventricular function and reserve: Progressive long-axis dysfunction with compensatory radial changes. Echocardiography 2011;28:813-20.
21. Hermans MP, Levy JC, Morris RJ, Turner RC. Comparison of insulin sensitivity tests across a range of glucose tolerance from normal to diabetes. Diabetologia 1999;42:678-87.
22. Zwanenburg JJ, Kuijer JP, Marcus JT, Heethaar RM. Steady-state free precession with myocardial tagging: CSPAMM in a single breathhold. Magn Reson Med 2003;49:722-30.
23. Chan SY, Brunken RC, Czernin J, Porenta G, Kuhle W, Krivokapich J, et al. Comparison of maximal myocardial blood flow during adenosine infusion with that of intravenous dipyridamole in normal men. J Am Coll Cardiol 1992;20:979-85.
24. Valenta I, Quercioli A, Vincenti G, Nkoulou R, Dewarrat S, Rager O, et al. Structural epicardial disease and microvascular function are determinants of an abnormal longitudinal myocardial blood flow difference in cardiovascular risk individuals as determined with PET/CT. J Nucl Cardiol 2010;17:1023-33.
25. DeGrado TR, Hanson MW, Turkington TG, Delong DM, Brezinski DA, Vallee JP, et al. Estimation of myocardial blood flow for longitudinal studies with 13N-labeled ammonia and positron emission tomography. J Nucl Cardiol 1996;3:494-507.
26. Gotte MJ, Germans T, Russel IK, Zwanenburg JJ, Marcus JT, van Rossum AC, et al. Myocardial strain and torsion quantified by cardiovascular magnetic resonance tissue tagging: Studies in normal and impaired left ventricular function. J Am Coll Cardiol 2006;48:2002-11.
27. Jacob JP, Vachier C, Morel JM, Daire JL, Hyacinthe JN, Vallee JP. Extrema temporal chaining: A new method for computing the 2D displacement field of the heart from tagged MRI. LNCS 2006;4179:879-908.
28. Cerqueira MD, Weissman NJ, Dilsizian V, Jacobs AK, Kaul S, Laskey WK, et al. Standardized myocardial segmentation and nomenclature for tomographic imaging of the heart: A statement for healthcare professionals from the Cardiac Imaging Committee of the Council on Clinical Cardiology of the American Heart Association. Circulation 2002;105:539-42.
29. Motivala AA, Rose PA, Kim HM, Smith YR, Bartnik C, Brook RD, et al. Cardiovascular risk, obesity, and myocardial blood flow in postmenopausal women. J Nucl Cardiol 2008;15:510-7.
30. Sela G, Landesberg A. The external work-pressure time integral relationships and the afterload dependence of Frank-Starling mechanism. J Mol Cell Cardiol 2009;47:544-51.
31. Chantler PD, Melenovsky V, Schulman SP, Gerstenblith G, Becker LC, Ferrucci L, et al. Use of the Frank-Starling mechanism during exercise is linked to exercise-induced changes in arterial load. Am J Physiol Heart Circ Physiol 2011;302:H349-58.
32. Cai H, Harrison DG. Endothelial dysfunction in cardiovascular diseases: The role of oxidant stress. Circ Res 2000;87:840-4.
33. Matsubara T, Dhalla NS. Relationship between mechanical dysfunction and depression of sarcolemmal Ca(2+)-pump activity in hearts perfused with oxygen free radicals. Mol Cell Biochem 1996;160-161:179-85.
34. Iwamoto T, Bai XJ, Downey HF. Coronary perfusion related changes in myocardial contractile force and systolic ventricular stiffness. Cardiovasc Res 1994;28:1331-6.
35. Deussen A, Brand M, Pexa A, Weichsel J. Metabolic coronary flow regulation—current concepts. Basic Res Cardiol 2006;101:453-64.
36. Gould KL. Assessing progression or regression of CAD: The role of perfusion imaging. J Nucl Cardiol 2005;12:625-38.
37. Schoenhagen P, Hachamovitch R, Achenbach S. Coronary CT angiography and comparative effectiveness research prognostic value of atherosclerotic disease burden in appropriately indicated clinical examinations. JACC Cardiovasc Imaging 2011;4:492-5.
38. Naya M, Murthy VL, Blankstein R, Sitek A, Hainer J, Foster C, et al. Quantitative relationship between the extent and morphology of coronary atherosclerotic plaque and downstream myocardial perfusion. J Am Coll Cardiol 2011;58:1807-16.

39. Carluccio E, Biagioli P, Alunni G, Murrone A, Leonelli V, Pantano P, et al. Advantages of deformation indices over systolic velocities in assessment of longitudinal systolic function in patients with heart failure and normal ejection fraction. Eur J Heart Fail 2011;13:292-302.
40. Moore CC, McVeigh ER, Zerhouni EA. Quantitative tagged magnetic resonance imaging of the normal human left ventricle. Top Magn Reson Imaging 2000;11:359-71.
41. Kramer CM, Malkowski MJ, Mankad S, Theobald TM, Pakstis DL, Rogers WJ Jr. Magnetic resonance tagging and echocardiographic response to dobutamine and functional improvement after reperfused myocardial infarction. Am Heart J 2002;143:1046-51.
42. Korosoglou G, Lossnitzer D, Schellberg D, Lewien A, Wochele A, Schaeufele T, et al. Strain-encoded cardiac MRI as an adjunct for dobutamine stress testing: Incremental value to conventional wall motion analysis. Circ Cardiovasc Imaging 2009;2:132-40.